

This is a repository copy of *Analysis of bondwires and RF compensation circuits in E-Band*.

White Rose Research Online URL for this paper: <a href="https://eprints.whiterose.ac.uk/id/eprint/233090/">https://eprints.whiterose.ac.uk/id/eprint/233090/</a>

Version: Accepted Version

#### Article:

Joseph, S.D. orcid.org/0000-0001-9756-7596 and Ball, E.A. orcid.org/0000-0002-6283-5949 (2025) Analysis of bondwires and RF compensation circuits in E-Band. IEEE Transactions on Components, Packaging and Manufacturing Technology, 15 (9). pp. 1986-1995. ISSN: 2156-3950

https://doi.org/10.1109/tcpmt.2025.3594505

© 2025 The Authors. Except as otherwise noted, this author-accepted version of a journal article published in IEEE Transactions on Components, Packaging and Manufacturing Technology is made available via the University of Sheffield Research Publications and Copyright Policy under the terms of the Creative Commons Attribution 4.0 International License (CC-BY 4.0), which permits unrestricted use, distribution and reproduction in any medium, provided the original work is properly cited. To view a copy of this licence, visit http://creativecommons.org/licenses/by/4.0/

# Reuse

This article is distributed under the terms of the Creative Commons Attribution (CC BY) licence. This licence allows you to distribute, remix, tweak, and build upon the work, even commercially, as long as you credit the authors for the original work. More information and the full terms of the licence here: https://creativecommons.org/licenses/

#### Takedown

If you consider content in White Rose Research Online to be in breach of UK law, please notify us by emailing eprints@whiterose.ac.uk including the URL of the record and the reason for the withdrawal request.



# Analysis of Bond Wires and RF Compensation Circuits in E Band

Sumin David Joseph, Member, IEEE and Edward A. Ball, Senior Member, IEEE

Abstract— This paper investigates the impact of bondwire interconnections on signal integrity in low and high millimeterwave (mmWave) applications, emphasizing transmission degradation caused by inductive and parasitic effects. Through detailed measurements and analysis, we demonstrate that transmission loss and impedance mismatches can be effectively reduced by minimizing bondwire length and using multiple wires in parallel. Based on empirical data, we developed an electrical model of bondwire incorporating distributed inductance, capacitance, resistance (L/C/R), and transmission characteristics. To further enhance performance, we introduce compact compensation circuits using LC structures and radial stubs optimized for both single and double bondwire configurations. Experimental validation shows that the proposed double-wire LC compensation technique significantly reduces insertion loss-from 5 dB to 1.5 dB and provides a return loss bandwidth from 70 GHz to 75 GHz. The key novelty of this work lies in integrating multiple bondwires with low-complexity, compact LC compensation structures, providing an effective solution for reducing insertion loss and improving impedance matching in mmWave systems. This approach offers a practical and scalable solution for improving chip-to-board and board-toboard interconnect performance in mmWave systems.

*Index Terms*— bond wire, compensation circuit, impedance matching, inductance, insertion loss, millimeter-wave, wire bonding.

# I. INTRODUCTION

N modern millimeter-wave communication systems, ensuring seamless connections between various components, particularly between monolithic microwave integrated circuits (MMICs) and off chip devices like antenna arrays, is crucial [1]. As wireless technologies continue advancing into higher frequency ranges, such as the E-band applications like 5G, automotive radar, and satellite communications demand high-performance and reliable interconnections [2]. Traditionally, bondwires have been widely used to connect MMICs to printed circuit boards (PCBs) due to their affordability and simplicity [3], [4]. However, when operating at millimeter-wave frequencies, bondwires can introduce significant performance limitations. The inductance and other parasitics due to bondwires and their pads degrade the interconnection and overall system performance. These challenges highlight the need for optimizing interconnects to preserve signal integrity and minimize losses [5].

This paragraph of the first footnote will contain the date on which you submitted your paper for review, which is populated by IEEE. This work was supported by the UKRI under Grant MR/T043164/1. *Corresponding author: Sumin David Joseph*).

The existing literature offers only a limited number of models for accurately characterizing bond wires. One such model, outlined in [6], utilizes a behavioral approach where the input impedance is derived from network analyzer measurements. In another method, Xue et al. [7] proposed a technique to model bond wires of various shapes through lumped element representations. Additional approaches, as presented in [8]–[10], involve directly computing S- and Y-parameters by employing causal equations or using the finite-difference timedomain (FDTD) technique. These sophisticated models accommodate more complex scenarios, such as non-uniformly shaped wires.

Achieving an effective wire-bonding interconnection for millimeter-wave applications is challenging due to the selfinductance of bondwires and the shunt capacitance associated with bond pads. Although some solutions have been developed for millimeter-wave applications, they typically involve complex designs, additional processing steps, and higher costs. In [11], a five-stage low pass filter technique is proposed for wideband interconnection. However, this technique incurs higher cost, large area and is incompatible for MMIC to PCB interconnections due to the asymmetric structure. Multiple signal lines from multiple bond pads are suggested in [12] and [13]. These techniques involve greater difficulty in implementation and use large area. Improvements in insertion loss and impedance matching have been achieved through the use of capacitive compensation structures, as noted in [14,15]. In [16] and [17], inductor-capacitor-inductor (LCL) structures with radial stubs are employed. LCL interconnects often fail to maintain consistent impedance, which is crucial for highfrequency signal transmission. Self-matching bondwires are proposed in [18] and [19], which uses long GSG wires for matching. Using GSG wires is challenging with thick PCBs as the matched wide microstrip does not leave space for the decoupling bondwires. In addition, stub matching is not always realistic as the stub width approaches its length for millimeterwave frequencies. LC planar matching at 60 GHz is presented in [20]. The compensation technique involves using additional bondwires for matching, which makes it complex to design. Also, it doesn't consider effect of multiple bondwires in the same pad area. Therefore, studies considering the possibilities of multiple bondwires are needed to address and reduce the difficulty in designing compensation and matching circuits [21-

The authors are with the School of Electrical and Electronic Engineering, University of Sheffield, UK, (e-mail: s.d.joseph@sheffield.ac.uk).

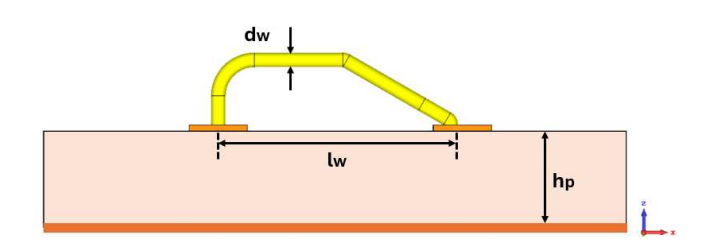


Fig. 1. Bond wire configuration.

In this study, we investigate the problems associated with bond wires in millimeter-wave applications and proposes compensation circuits for improving the matching. The key contributions of this paper are as follows:-

- Detailed measurement and analysis of single and multiple bondwires in mmWave bands (22-32 GHz and 68-76 GHz).
- Developed a novel electrical model of the bondwire that incorporates distributed L,C,R and transmission lines, based on measured data.
- Design and analysis of compact transmission lines LC and radial stub compensation to mitigate transmission loss and impedance mismatches in bondwire interconnects.
- Introduced a novel, low-complexity compensation approach that combines multiple parallel bondwires with compact LC structures.

The selected frequency bands 22–32 GHz and 68–76 GHz (Eband)—are increasingly recognized as critical in mmWave research due to the applications in 5G and 6G networks [24]. This paper is organized as follows: Section II discusses the modeling of the bondwire, and the analysis of the bond wire is carried out in Section III. Section IV presents the equivalent circuit based on the measured results. Sections V discusses the design of bond compensation structure and measurement results of compensated bondwire is presented in Section VI. Finally, Section VII presents the conclusions.

# II. BOND WIRE MODELING

A bond wire can generally be modeled as an inductor along with various parasitic components. Full-wave electromagnetic simulation techniques, like the method of moments and the finite-difference time-domain approach, are used to thoroughly evaluate various bond wire configurations, including multichip setups as well as single and double bond wire structures. Configuration of a single bondwire for interconnecting chips to PCB board can be shown as in Fig. 1. The geometric dimensions of the bond wires are defined as follows: d represents the wire's diameter,  $l_w$  is the wire's length, h denotes the height of the wire and  $h_p$  refers to the thickness of the substrate material. The bondwire's equivalent circuit can be represented as a low-pass filter network comprising a series inductance (Ls), a series resistance (Rs), and parallel capacitances (*Cp*) to ground, as illustrated in Fig. 2. The values of Ls and Cp can be estimated using equations (1) and (2), respectively, based on the geometric and material parameters of the bondwire [15].

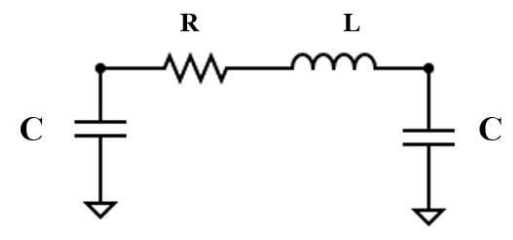


Fig. 2. Conventional bond wire equivalent circuit.

$$L_s = (\mu_0 l_w / 2\pi) [\ln(4l_w / d_w) + \mu_r \tan(4l_w / d_w) - 1]$$
 (1)

$$C_p = \varepsilon_r \varepsilon_0 (A/h_p) \tag{2}$$

$$R_s = (4\rho l_w/\pi d_w^2) \cos(0.025 d_w/d_s + 0.2654)$$
 (3)

where  $\mu_0$  and  $\varepsilon_0$  are the permeability and the permittivity of free space, respectively,  $\mu_r$  and  $\varepsilon_r$  are the permeability and the permittivity of bond wire, respectively, and  $\rho$  and ds are the resistivity and skin depth of the bond-wire material, respectively. A is the area of the bonding pads of the wire in (2). The inductance  $L_s$  of the bond wire is a key factor in determining its microwave performance. To model and analyse the microwave behaviour of bond wire interconnections, a combined approach using ADS and electromagnetic field simulation software CST are employed.

In this study, a gold bond wire with a diameter of 25  $\mu m$  is initially designed. The bond wire pads measure 100  $\mu m$  in length and 450  $\mu m$  in width and are designed with a characteristic impedance of 50  $\Omega$  to ensure proper impedance matching. The distance between the bond wire pads is 320  $\mu m$ , with a 40  $\mu m$  offset on both ends of the wire relative to the pad edges. Consequently, the total length of the bond wire is calculated to be 480  $\mu m$ . For this investigation, a low-loss Rogers RO4003C substrate, 200  $\mu m$  thick, is chosen. Additionally, a copper ground plane is positioned on the opposite side of the substrate.

The bond wire configuration in Fig. 1 was initially simulated in the frequency range of 20 to 80 GHz to assess its performance in millimeter-wave application. The simulation was carried out using CST Microwave Studio, where waveguide ports were

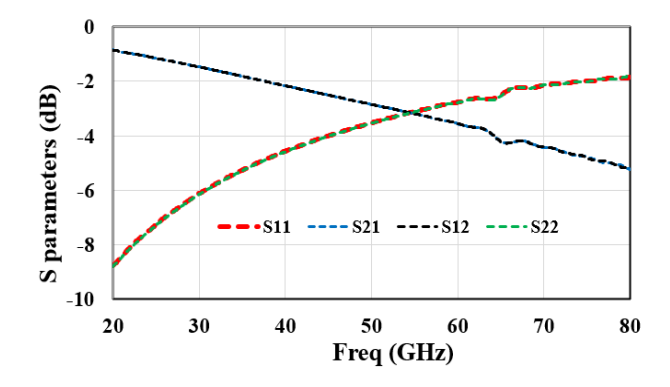


Fig. 3. Simulated S parameters of bondwire in millimeterwave frequencies .

assigned to both ends of the bond wire pads to excite and terminate the structure. The layout includes the bond wire, its associated pads, and surrounding ground, ensuring that the simulation closely mirrors the physical setup, excluding realworld imperfections. Fig. 3 shows the simulated S parameters of bondwire. The results show a degradation in the transmission characteristics as the frequency increases, largely due to the inductive effects of the bond wire. The insertion loss degrades from an initial value of less than 1 dB at 20 GHz to 5 dB at 80 GHz. Similarly, the reflection coefficient was around -9 to -6 dB in the low millimeter-wave region. However, the reflection coefficient rises to -2 dB in the E band region. Therefore, it can be observed that the bond wire does impact severely in the lower millimeter-wave region. Therefore, it becomes crucial to account for the parasitic effects of the bond wire and apply appropriate compensation to improve impedance matching and enhance transmission performance.

#### III. ANALYSIS OF BOND WIRES

In order to assess the performance of bond wires at millimeter-wave frequencies, a printed circuit board (PCB) was designed utilizing a low-loss Rogers RO4003C substrate. This material has a permittivity of  $\epsilon_{\rm r}=3.55,$  a loss tangent of 0.0027, and a thickness of 200  $\mu m.$  The PCB includes pads designed for varying bond wire lengths. Additionally, Through, Reflect, Line (TRL) calibration standards were integrated onto the chip to remove the effects of the Ground-Signal-Ground (GSG) probe transition during testing.

For the bond wire fabrication, a semi-automatic wedge bonder, iBond5000, was employed. A single gold bond wire

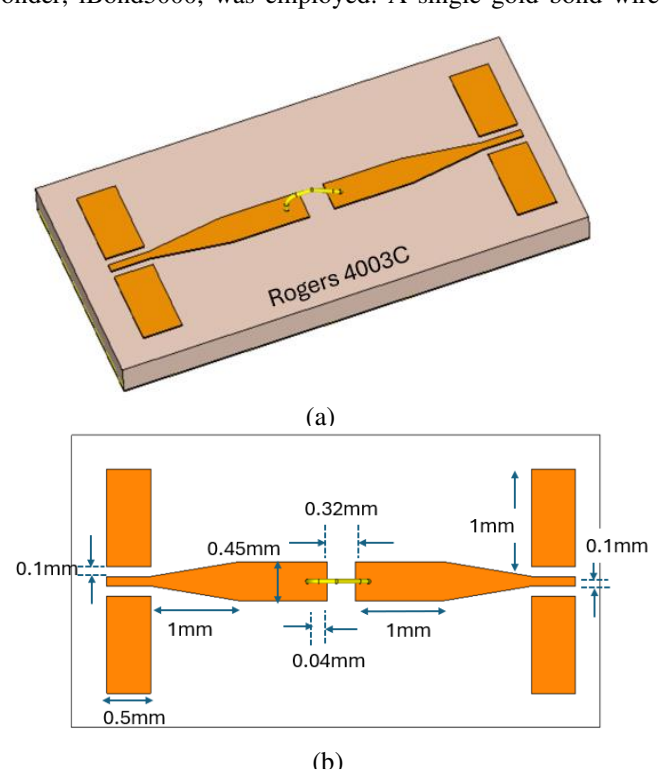


Fig. 4. Bond wire schematic (a) perspective view (b) top view.

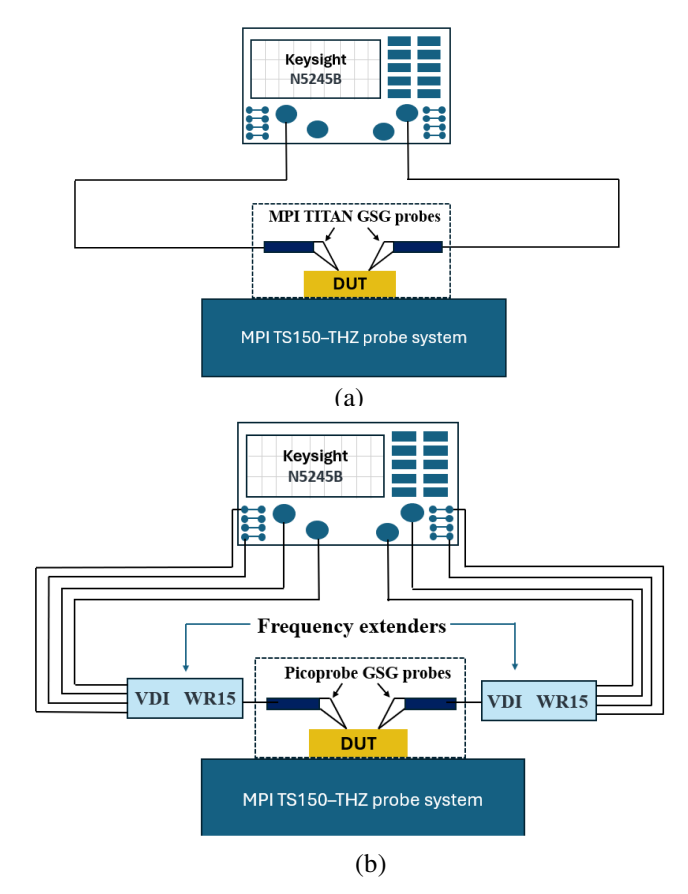


Fig. 5. Measurement set up of bondwire (a) low frequency (24-30GHz) (b) high frequency (70-75GHz).

with an overall length of 480  $\mu m$  was initially fabricated, as shown in the Fig. 4. The bond wire pads were designed with dimensions of 100  $\mu m$  in length and 450  $\mu m$  in width, and a characteristic impedance of 50  $\Omega$  to ensure proper impedance matching. To connect the bond wire to the GSG pads, which have a 150  $\mu m$  pitch, a 1 mm microstrip line with a tapering section was added on both sides of the wire. The bond wire pads were spaced 320  $\mu m$  apart, with a 40  $\mu m$  offset from the edges of the pads to each end of the bond wire (representing typical manufacturing techniques). This configuration resulted in an overall bond wire length of 480  $\mu m$ . The fabricated bond wire is depicted in the accompanying figure.

Initial analyses were conducted in the lower millimeter-wave frequency range at the UKRI Millimeter Wave Laboratory at the University of Sheffield (TUoS) [25]. Fig. 5(a) shows the schematic diagram of the low frequency measuremnt set up. The performance of the bond wire was measured over the 24 to 30 GHz frequency range using a Keysight PNA-X N5245B network analyzer and MPI Titan RF probes with a 150  $\mu m$  pitch. Fig. 6 shows the fabricated single and triple bondwire. The simulated and measured results of single bond wire in the low frequency region is shown in Fig. 7(a). The measured results indicate that the insertion loss ranges from 0.8 dB to 2 dB, which aligns well with the simulated values. Similarly, the measured S11 varies between -9.7 dB and -6.5 dB across the frequency range. A noticeable degradation in transmission

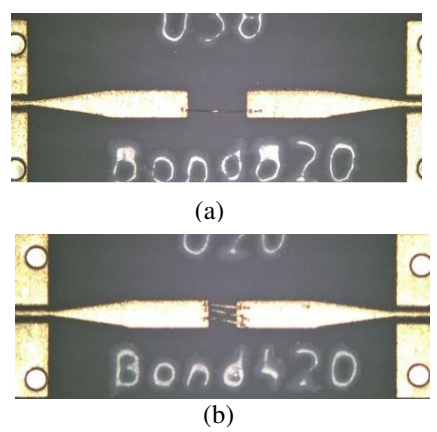


Fig. 6. Fabricated (a) ) single bond wire with overall length  $820 \mu m$  (b) triple bond wire with overall length  $480 \mu m$ 

performance and impedance matching is observed as the frequency increases, primarily due to the inductive properties of the bond wire. To address this issue, the performance of multiple bond wires is analyzed at lower millimeter-wave frequencies by implementing triple wire bonds, as shown in Fig. 6(b). The S-parameter results for the triple bond wire configuration are presented in Fig. 7(b). The insertion loss is significantly reduced—from 0.1 dB at 22 GHz to 0.6 dB at 35 GHz. Similarly, the return loss improves, indicating better impedance matching, with values ranging from -15 dB to -13 dB across the frequency band. These results demonstrate that, at lower millimeter-wave frequencies, the use of multiple bond wires can effectively reduce signal losses and enhance overall performance.

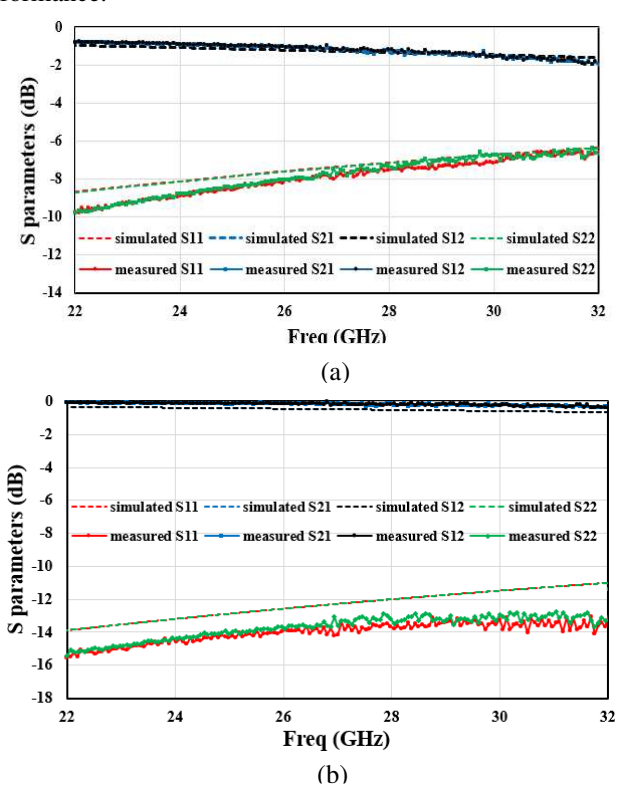


Fig. 7. Simulated and measured S parameters of 480  $\mu$ m (a) single bond wire (b) triple bondwire in low mmWave band.

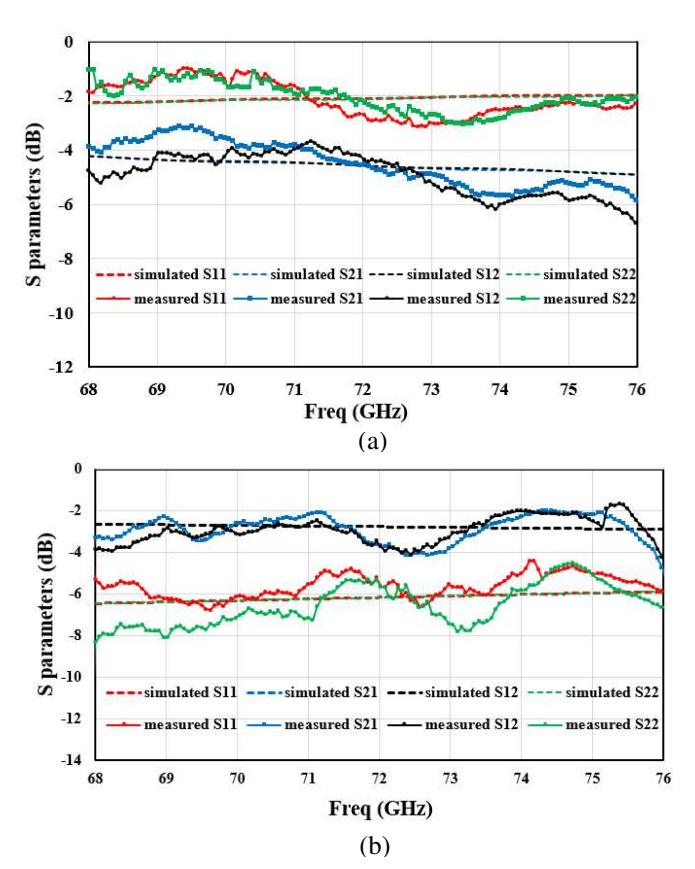


Fig. 8. Simulated and measured S parameters of 480  $\mu$ m (a) single bond wire (b) triple bondwire in high mmWave band.

For analysing the transmission performance in bondwires at high frequency millimeter-wave bands, WR15+ VDI extenders are used along with the PNA as shown in Fig. 5(b). Fig. 8(a) shows the simulated and measured S parameter results of the single bondwire. The transmission characteristics are degrading with frequency due to the inductive effect. Around 73 GHz, it is possible to observe insertion loss value of around 4 to 6 dB compared to less than 2 dB at 35 GHz. Similarly, the return loss curves are degraded to 2 dB range. Therefore, it is necessary to design compensation circuits and matching networks to reduce the losses and to improve matching.

Triple wire bond performance at high millimeter-wave frequencies are shown in Fig. 8(b). Insertion loss is reduced to 3

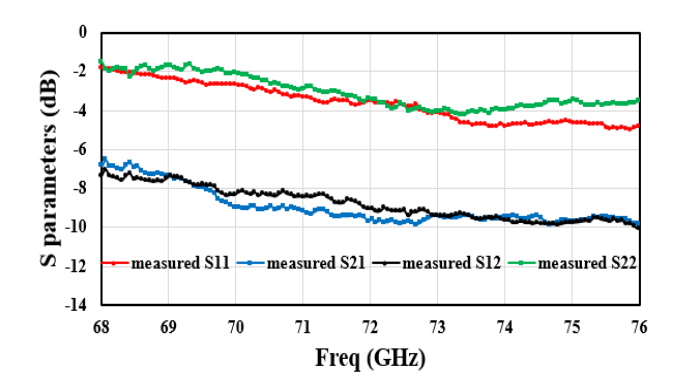


Fig. 9. Measured S parameters of bond wire with overall length 880 μm in high millimeter-wave frequency band.

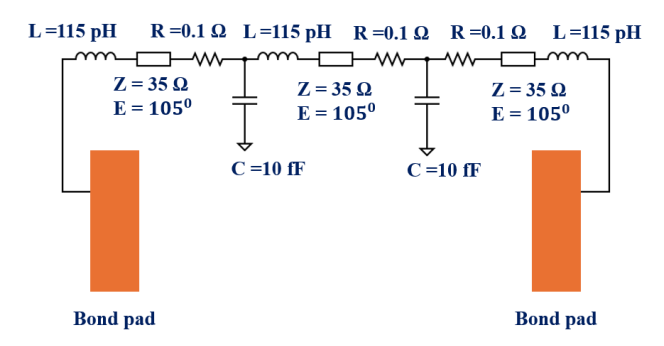
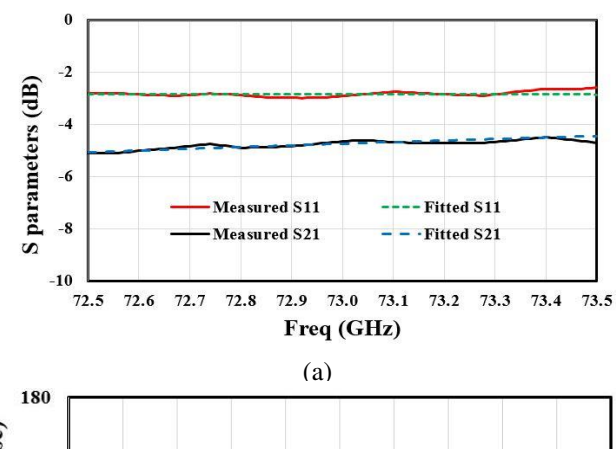


Fig. 10. Estimated bondwire equivalent circuit.

dB range and return loss to circa 7 dB. However in high frequencies, it is necessary to use compensation and matching circuits to achieve good transmission performance. Fig. 9 shows the measured results of 880 μm long single bond wire. Compared to 480 μm long bondwire, this scenario has high transmission loss of around 9 dB. Thus, it is required to minimise the bondwire length interconnects wherever possible.

#### IV. EQUIVALENT CIRCUIT

To evaluate the measured bondwire results and to design compensation network, it is necessary to estimate the equivalent circuit of the bondwire. In this work, a fitted model is used to analyze the S parameters at the high millimeter-wave frequency band. Measurement results of standard bondwire with an overall length of 480  $\mu$ m is utilized. The dembedded results of the bond pad and bondwire are fitted with an equivalent circuit at 73 GHz as



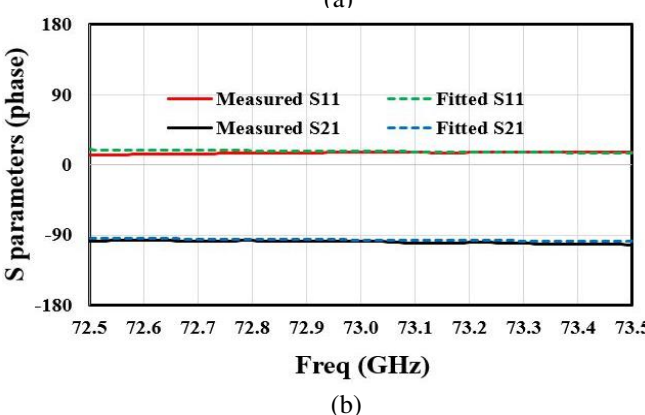


Fig. 11. S parameter of measured bondwire with 480  $\mu$ m bondwire and fitted results

shown in Fig. 10. A distributed model is used with inductance L, resistance R, ideal transmission line with electrical length E and impedance Z, along with parallel capacitance C. Distributed model with transmission line can incorporate the delay and phase values associated with bondwire, as the length of bondwire is comparable with wavelength. The inductance L of 115 pH is extracted in each section giving an overall inductance of 345 pH. This value is similar to the simulated values with this length and operating frequency. Equivalent circuit parallel capacitance values are reasonably low as we already considered and include the capacitance of bond pads through EM simulations in ADS.

The proposed lumped element combined with transmission line equivalent circuit shown in Fig. 10 remains a valuable and insightful approach for modeling bond wires, particularly in the higher millimeter-wave frequency range, when applied over narrow bandwidths. Within these constrained frequency spans, the model can accurately capture key effects such as inductance, resistance, and localized transmission behavior. This modeling strategy is especially useful for analyzing resonant structures, matching networks, and interconnect transitions where bandwidth is limited, and where quick, circuit-level interpretation is essential. However, due to the increasingly distributed nature of bond wires at higher frequencies, along with effects like radiation, parasitics, and skin effect, the model's accuracy naturally diminishes over wider bandwidths. These high-frequency phenomena are more full-wave electromagnetic appropriately captured using simulations or wideband behavioral models. Nonetheless, for targeted applications and narrowband analysis, the lumped element + transmission line equivalent circuit continues to offer a practical and sufficiently accurate solution for bond wire modeling in the millimeter-wave regime.

#### V. COMPENSATION CIRCUIT DESIGN

While designing compensation circuits for bond wire parasitics, it is necessary to design asymmetric networks to enable the technique suitable for commercial high frequency circuits and RF chips. A transmission line-based asymmetric matching network is initially designed at the schematic level to avoid the need for repetitive and time-consuming 3D electromagnetic simulations. The bondwires and their landing pads are considered together; therefore, the landing pads are not part of the compensation circuit.

# A. Radial Stub Compensation Design

To mitigate the series inductance introduced by bond wire connections, a capacitive radial stub is integrated alongside a narrow microstrip line serving as an impedance transformer as in Fig. 12. Initial design parameters, such as the stub's radius and angular span, are derived through preliminary simulations using

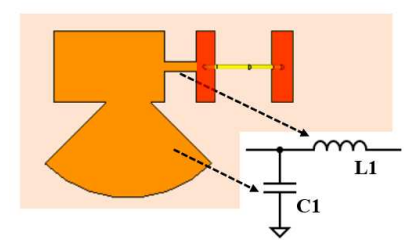


Fig. 12. Layout of radial stub compensation structure for higher millimeter wave bands

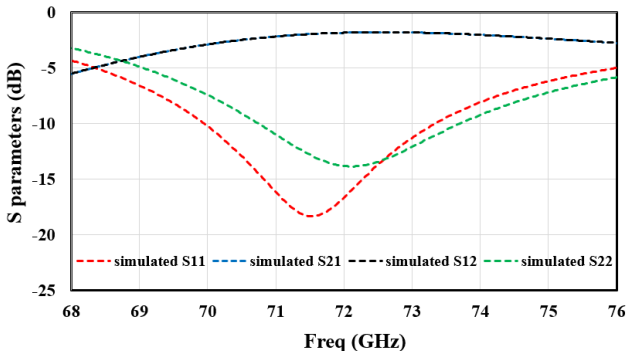


Fig. 13. Simulated S parameter with radial stub compensation and bondwire at high millimeter-wave bands

Keysight ADS. These parameters are then fine-tuned using full-wave electromagnetic CST simulation to ensure effective impedance compensation and improved signal transmission. Fig. 13 shows the S parameter results of compensation circuit.

# B. Low Frequency LC Transmission Lines Compensation

The use of a multistage network offers greater design flexibility, enabling the implementation of scenarios where large values for individual matching components may be challenging to achieve in the physical layout. In transmission line-based matching, thick metal traces can provide capacitance against the ground plane and thin metal traces form inductors in microstrip PCB, as follows [26]:

$$C = \varepsilon_r \varepsilon_0 \left( \frac{l_t \times w_t}{h_p} \right) \tag{4}$$

$$L = \frac{\ln\left(\frac{8hp}{w_t} + \frac{w_t}{4hp}\right) 60l_t}{v} \qquad \frac{w_t}{h_p} \le 1$$

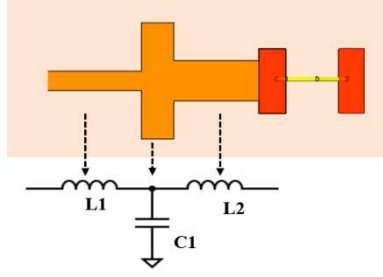


Fig. 14. Layout of LC transmission lines compensation structure for lower millimeter-wave bands

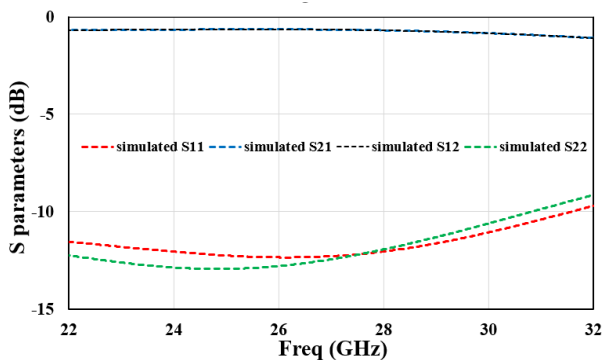


Fig. 15. Simulated S parameter results with LC compensation and bondwire at low millimeter-wave bands

$$= \frac{120\pi l_t}{v\left(\frac{w_t}{h_D} + 1.39 + 0.66 \ln\left(\frac{w_t}{h_D} + 1.44\right)\right)} \frac{w_t}{h_D} \ge 1 \quad (5)$$

where  $l_t$  and  $w_t$  are the length and width of the trace and v is the wave-propagation velocity. These equations provided firstorder estimates of the inductance (L) and capacitance (C) of microstrip line segments based on basic geometric and material parameters. They were useful for the initial design and impedance matching of microstrip lines. Later, electromagnetic (EM) simulation tool CST was used for finetuning and more accurate optimization. To model the transmission line behavior of planar PCB traces (microstrip lines) for impedance matching, equations (4) and (5) were applied—where equation (4) estimated the parasitic capacitance between the trace and ground, and equation (5) calculated the inductance based on the trace geometry and substrate height. In this low-frequency LC transmission line compensation approach, two equivalent inductors and one capacitor are realized using transmission lines, as shown in Fig. 14 for impedance matching. A low-value inductor L2 is placed near the bondwire, followed by a thick metal section that acts as the capacitor C1, and then a larger inductor L1. In low frequency compensation, the lengths of the microstrip lines lt1, lt2 and lt3 are 0.59, 0.2 and 0.51 mm respecitvely. Width wt1, wt2 and wt3 are 0.12, 0.73 and 0.25 mm respectively. This arrangement forms a T-shaped matching network that provides effective impedance matching. Fig. 15 shows the simulated S parameters of the low frequency LC transmission lines compensation. A broadband impedance matching covering 22-32 GHz can be observed with insertion loss less than 1dB.

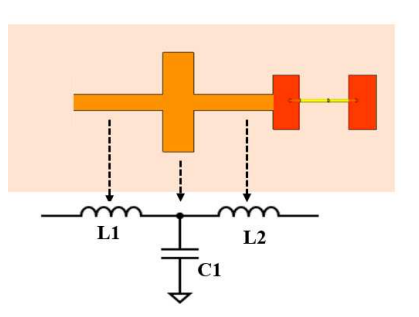


Fig. 16. Layout of LC transmission lines compensation structure for higher millimeter-wave bands

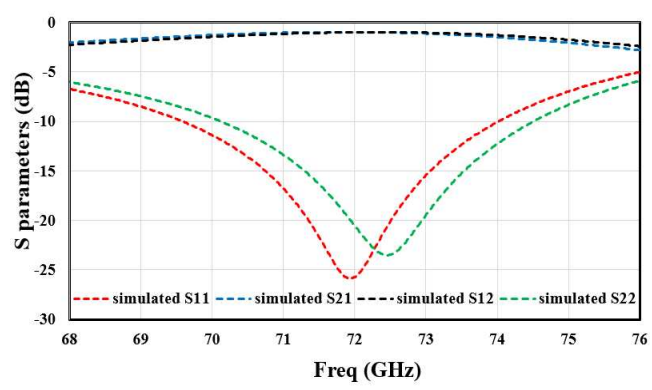


Fig. 17. Simulated S parameter results with LC compensation and bondwire at high millimeter-wave bands

#### C. High Frequency LC Transmission Lines Compensation

A similar T-shaped impedance matching circuit was employed for high-frequency compensation, with modified transmission line dimensions is shown in Fig. 16. Two thin metal traces with widths  $w_{tl} = w_{t3} = 0.12$  mm were used as inductors, while a thicker trace  $w_{t2} = 0.7$  mm acted as the shunt capacitor. The lengths of the three microstrip lines were  $l_{tl}$ ,=0.58,  $l_{t2}$ =0.2 and  $l_{t3}$  0.51 mm, respectively. This compensation network provided effective wideband impedance matching and minimized insertion loss introduced by the bond wire. Fig. 17 shows the simulated S-parameters of the high-frequency LC transmission line network. Wideband impedance matching (S11<-10 dB) was achieved between 70 and 74 GHz, with an insertion loss of less than 1.5 dB across this range. Compared to a radial stubbased approach, the T-shaped matching circuit demonstrated superior performance.

# D. Double Bondwire LC Compensation

As observed in Section III, uncompensated interconnects with multiple bond wires demonstrated comparatively better performance. Building on this, the proposed compensation technique was further applied using a double bond wire configuration. The use of two bond wires in parallel effectively reduces the overall inductance, thereby lowering the insertion loss. This makes the compensation implementation simpler and more efficient compared to the single bond wire scenario. The compensation circuit, shown in Fig. 18, employs a single inductive and capacitive microstrip trace. The capacitive strip has dimensions  $l_{tl}$  =0.1 mm and  $w_{tl}$  = 0.7mm, while the inductive strip has a length  $l_{t2}$  =0.5 mm and width  $w_{t2}$  = 0.12 mm. Fig. 19 presents the simulated S-parameters of the double bond wire compensation network. A broad bandwidth covering the full frequency range of interest (66-76 GHz) was achieved, with a simulated insertion loss of less than 1dB across this band.

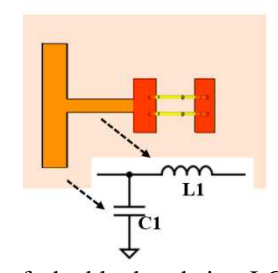


Fig. 18. Layout of double bondwire LC compensation structure for higher millimeter-wave bands

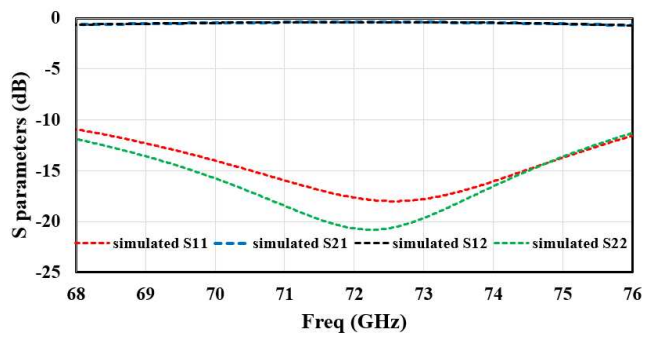


Fig. 19. Simulated S parameter results with double bondwire LC compensation at high millimeter-wave bands

#### VI. MEASUREMENT RESULTS

The proposed compensation circuits were fabricated on a Rogers 4003C substrate with a thickness of 200  $\mu m$ . Bond wires with a length of 480  $\mu m$  and a diameter of 25  $\mu m$  were implemented on the boards using an i5000 wedge bonder. The measurement setups shown in Fig. 5(a) and Fig. 5(b) were used to evaluate the S-parameter performance in the low- and high-frequency bands, respectively.

# A. Radial Stub Compensation Results

Fig. 20(a) shows the fabricated radial stub compensation circuit implemented with a single bond wire of 480 μm length. The measured S-parameters of the bond wire interconnect with radial stub compensation, spanning 68 to 76 GHz, are presented in Fig. 20(b). The measured return loss exceeds 10 dB in the 71.5 to 74 GHz range. However, the insertion loss remains below 3.5 dB only in the 72.5 to 74 GHz range, representing a minor improvement compared to the uncompensated case shown in Fig. 8(a). Thus, while the addition of the capacitive radial stub improves impedance matching by partially cancelling the inductive effect of the bond wire, it offers only limited enhancement in insertion loss and results in narrowband performance.

## B. Low Frequency LC Txion Lines Compensation Results

The fabricated low frequency LC txion lines compensation circuit is shown in Fig. 21 (a). Measured S parameters of the bond wire interconnect with compensation circuit from 22 to 32 GHz is shown in Fig. 21(b). Simulated and measured results are in well agreement. It can be observed that the insertion loss is reduced to between 0.1 to 1 dB in the wideband compared to the 0.5 to 2.1 dB insertion loss in the bond wire interconnect without compensation as shown in Fig. 7(a). The impedance matching performance is very much improved from 22 to 32 GHz. The

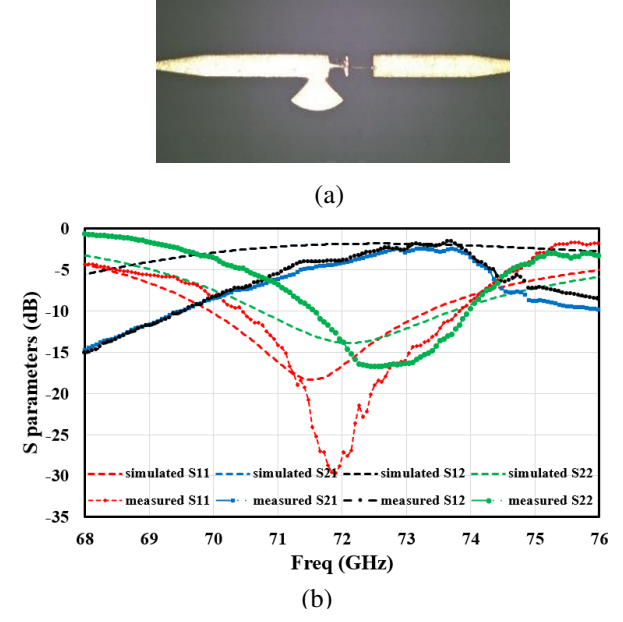


Fig. 20. (a) Microscopic image of radial stub compensation interconnects at high bands (b) measurement results

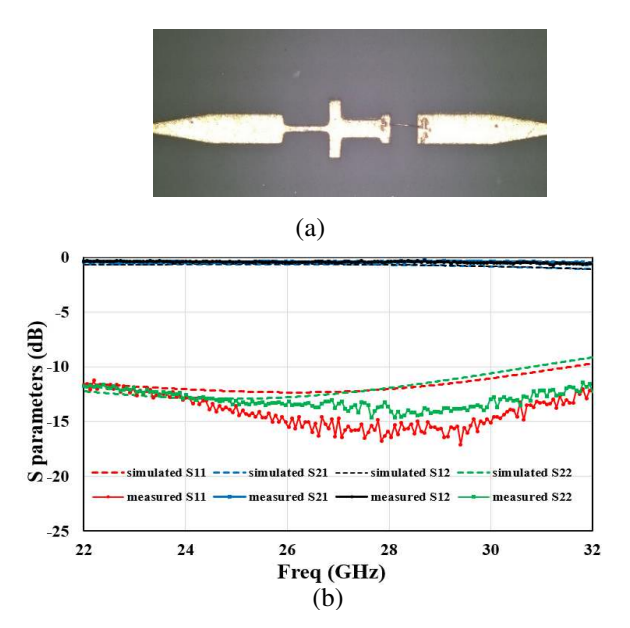


Fig. 21. (a) Microscopic image of LC lines compensated interconnects at low bands. (b) measurement results

return loss curves S11 and S22 are also better than 10 dB throughout the band. At 28 GHz, the return loss curves are improved from 8 to 15 dB. Therefore, we see that to improve the impedance matching performance with bond wire degradation, it is possible to either using multiple bond wires or by using the proposed compensation circuit in low millimeter-wave region.

# C. High Frequency LC Txion Lines Compensation Results

The fabricated high frequency compensation circuit centered at 73 GHz is shown in Fig. 22 (a). Fig. 22(b) presents the measured performance of the LC compensation circuit with a single bond wire. Compared to the radial stub compensation, a significant improvement in impedance matching was observed. The

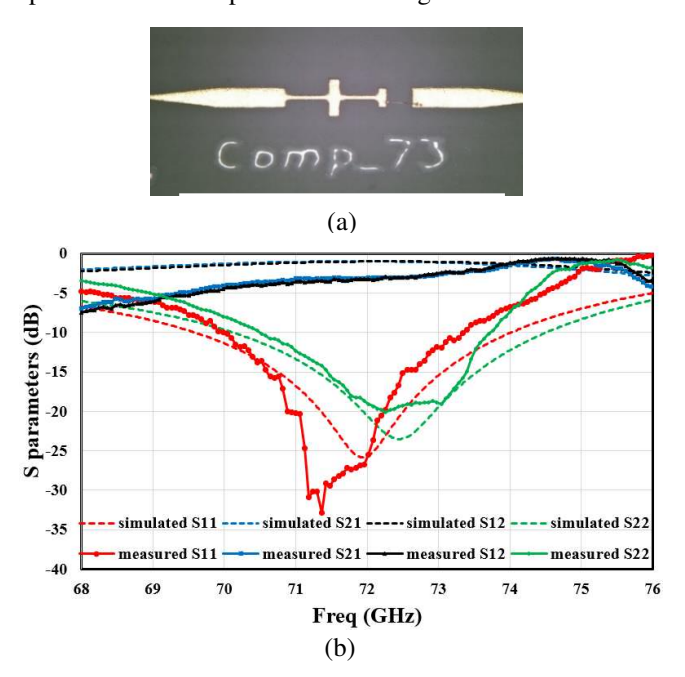


Fig. 22. (a) Microscopic image of LC lines compensated interconnects at high bands. (b) measurement results

measured return loss bandwidth extends from 70.5 to 73.5 GHz, with a minimum insertion loss of  $2.2~\mathrm{dB}$  at 73 GHz. The measured insertion loss is slightly higher than the simulated result, likely due to PCB etching tolerances and a longer-than-expected bond wire. Nonetheless, both return loss and insertion loss show substantial improvement within the 70.5–73.5 GHz band, with insertion loss ranging from  $3.2~\mathrm{dB}$  to  $1.6~\mathrm{dB}$ .

# D. Double Bond Wire Compensation Results

Finally, the double bond wire configuration with LC compensation was fabricated, as shown in Fig. 23(a). The measured S-parameter performance is presented in Fig. 23(b). It can be observed that the insertion loss (S21 and S12) is significantly improved, reaching as low as 1.2 dB at 72 GHz. Additionally, the return loss remains better than –10 dB across the 70–75 GHz frequency range. Within this 5 GHz bandwidth, the insertion loss stays below 1.5 dB. These results demonstrate that the LC-compensated double bond wire structure offers superior performance compared to the single bond wire approach. This improvement is primarily attributed to the reduced interconnect inductance achieved by using multiple bond wires in parallel. As a result, a simple LC-based impedance matching circuit is sufficient to enhance the transmission performance of bond wire interconnects.

Despite the high performance, a decrease in bandwidth performance can be observed compared to simulated curves. These discrepancies are attributed to practical factors such as fabrication tolerances, variations in wire bond geometry (e.g., loop height and angle), and probe contact inconsistencies, which are not fully captured in the simulation environment. In particular, for the double wire compensation case, the mismatch between simulation and measurement is slightly higher due to the difficulty in achieving two perfectly parallel wires in practice, as assumed in the simulation. This is mainly because

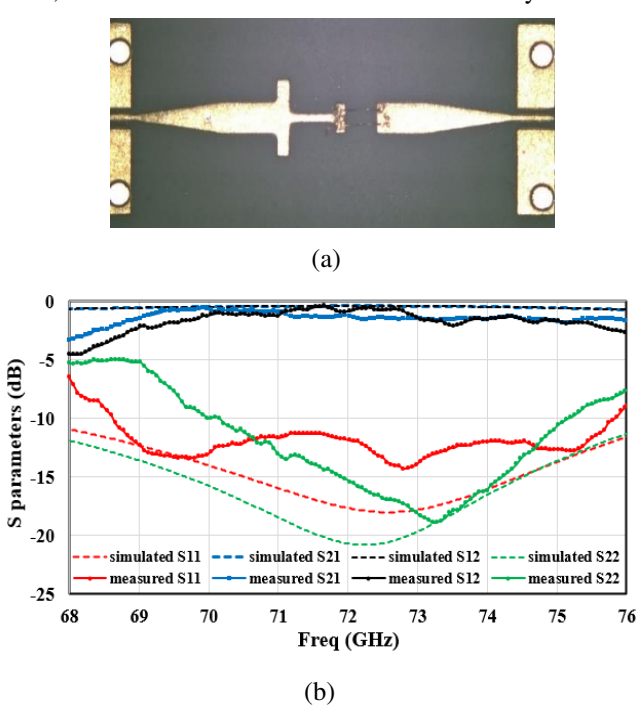


Fig. 23. (a) Microscopic image of LC lines compensated double wire at high bands (b) measurement results

Ref	Technique used	Operating Frequency (GHz)	Insertion loss	Return loss	Complexity	Single/ multiple bonds
[11]	Transmission lines- based LC combined with ground pad C on both sides	80	0.4 dB at 76 GHz	15	Incompatible for chips	Only double bonds
[13]	Three-path interconnect and ground bond pad	92	2dB at 70 GHz	13	Very complex	Single signal lines from each 3 bond pads
[12]	Two-path interconnect and ground bond pad	84	3 dB at 84	13.4	Very complex	Single signal lines from each 2 bond pads
[14]	Comb capacitors attached to bonding pads	5	-	8	Very complex	Single bonds
[16]	LCL structure	60	1.7 at 52	18	Complex due to multiples wires as GSG	Triple bonds and radial stubs in IC (LCL structure)
[17]	LCL structure as T network	60	3.1		Multiple double wires as GSG with open stub	Double bond wires in parallel and open-ended stubs
[18]	Self match length	120	1.5		Parallel long GSG	GSG wires with matching
[20]	LC planar lumped	70	1.5	14	Moderate -using additional bondwires	Single wire with compensation
[19]	Series stub	123	1.5	15	GSG wires with	GSG wires with matching

TABLE I
COMPARISON OF THIS WORK WITH OTHER RELEVANT WORKS

the bonding process is semi-automatic, leading to slight variations in wire placement and geometry.

73

1.5

15

Simple LC

matching

**Transmission Lines** 

**LC Compensation** 

**This** 

work

The results of the bondwire interconnection measurements, along with their analysis, are summarized and compared with the current state-of-the-art in Table I. Symmetric matching is incompatible with chip-to-board transitions since adjustments can only be made at the board level. Thus, the symmetric works in [11] is not suitable for these transitions. Implementing Ground-Signal-Ground (GSG) bondwires is challenging when using thick PCBs, as the matched wide microstrip leaves insufficient space for adjacent decoupling bondwires [18],[20]. Large bonding pads and multiple signal and ground lines are required in [12],[13] designs, which makes it very complex to implement. Furthermore, stub matching is often impractical at mmWave frequencies, as the stub width may approach its length. LCL interconnects frequently struggle to maintain consistent impedance, which is essential for reliable highfrequency signal transmission [16],[17]. The inductance introduced by the bondwire can disrupt impedance matching, particularly at mmWave frequencies, leading to signal reflections, power loss, and attenuation.

This proposed work presents the first asymmetric double bondwire compensation approach, whereas most other studies have used either single bondwires or multiple bondwires with complex stubs or grounded pads. Complexity and design risk of this design procedure is reasonably low compared to other works. In this work, we have explored the possiblity of multiple bondwires in the same pad area along with asymmetric compensation networks, which makes it very viable for chip to board transitions. We propose a new electrical model for bond wires, using a distributed L/C/R + transmission line concept. While some wirebonding systems use ribbon bonds to reduce parasitic inductance, not all wirebonder equipment supports this technique. In contrast, all commercial wirebonding systems are capable of supporting multiple wire bonds. Therefore, we believe our multiple wire bond approach is more generic and broadly applicable in both industry and academia, offering a practical and scalable solution.

Double wire with

compensation

#### VII. CONCLUSION

This work investigated the challenges associated with bondwire interconnections in both low and high mmWave frequency applications, focusing on signal degradation caused by inductive and parasitic effects. Through comprehensive measurements and analysis, it was demonstrated that transmission loss and impedance mismatches can be significantly mitigated by minimizing bondwire length and employing multiple bondwires in parallel. An accurate electrical model of the bondwire interconnect was developed, incorporating distributed inductance, capacitance, resistance

(L/C/R), and transmission line behavior based on empirical data. To further enhance performance, compact impedance compensation circuits—based on radial stubs and LC structures —were designed and implemented for single and double bondwire configurations. Experimental validation using standard 25 µm diameter gold bondwires confirmed the effectiveness of the proposed techniques. Specifically, the double bondwire LC-compensated interconnect achieved a reduction in insertion loss from 5 to 1.5 dB, with the return loss bandwidth extended over the 70 to 75 GHz range. These results demonstrate notable improvements in signal integrity and impedance matching, validating the proposed approach. To the best of our knowledge, this work presents one of the most compact, low-complexity, and effective solutions for mitigating bondwire-induced degradation in mmWave chip-to-board and board-to-board interconnects by integrating multiple bondwires with low-complexity, compact LC compensation structures.

# ACKNOWLEDGMENT

The authors acknowledge the measurement support from the UKRI National millimeter wave Measurement Facility [25]. This research was funded by UKRI, grant number MR/T043164/1.

#### REFERENCES

- [1] T. S. Rappaport et al., "Millimeter wave mobile communications for 5G cellular: It will work!" *IEEE Access*, vol. 1, pp. 335–349, 2013.
- [2] S. Beer et al., "Design and measurement of matched wire bond and flip chip interconnects for D-band system-in-package applications," in *Proc. IEEE MTT-S Int. Microw. Symp.*, Jun. 2011, pp. 1–4.
- [3] H. Y. Lee, "Wideband characterization of a typical bonding wire for microwave and millimeter-wave integrated circuits," *IEEE Trans. Microw. Theory Technol.*, vol. 43, no. 1, pp. 63–68, Jan. 1995.
- [4] C. Schuster, G. Leonhardt, and W. Fichtner, "Electromagnetic simulation of bonding wires and comparison with wide band measurements," *IEEE Trans. Adv. Packag.*, vol. 23, no. 1, pp. 69–79, Feb. 2000.
- [5] S. R. Zahran et al., "Bondwire Integration Challenges in E-band Systems: from PCB to Die Level," in *Proc. Eur. Microw. Conf.*, Berlin, Germany, pp. 846-849, 2023.
- [6] T. P. Wang and Y. F. Lu, "Fast and accurate frequency-dependent behavioral model of bonding wires," *IEEE Trans. Ind. Inform.*, vol. 13, no. 5, pp. 2389–2396, Oct. 2017.
- [7] H. Xue, C. R. Benedik, X. Zhang, S. Li, and S. Ren, "Numerical solution for accurate bondwire modeling," *IEEE Trans. Semicond. Manuf.*, vol. 31, no. 2, pp. 258–265, May 2018.
- [8] A. L. Nazarian et al., "A physics-based causal bond-wire model for RF applications," *IEEE Trans. Microw. Theory Techn.*, vol. 60, no. 12, pp. 3683–3692, Dec. 2012.
- [9] W. Tian, H. Cui, and W. Yu, "Analysis and experimental test of electrical characteristics on bonding wire," *Electron.*, vol. 8, no. 3, 2019.
- [10] F. Alimenti, P. Mezzanotte, L. Roselli, and R. Sorrentino, "Modeling and characterization of the bonding-wire interconnection," *IEEE Trans. Microw. Theory Techn.*, vol. 49, no. 1, pp. 142–150, Jan. 2001.
- [11] T. P. Budka, "Wide-bandwidth millimeter-wave bond-wire interconnects," IEEE Trans. Microw. Theory Techn., vol. 49, no. 4, pp. 715–718, Apr. 2001
- [12] C.H. Li, C.L. Ko, C.N. Kuo, M.C. Kuo, and D. C. Chang, "A low-cost DC-to-84-GHz broadband bondwire interconnect for SoP heterogeneous system integration," *IEEE Trans. Microw. Theory Techn.*, vol. 61, no. 12, pp. 4345–4352, Dec. 2013.
- [13] W.M. Wu, M.C. Yu, C.H. Li, and C.N. Kuo, "A low-cost DC to-92 GHz broadband three-path bondwire interconnect," in *Proc. IEEE Int. Symp. Radio-Freq. Integr. Technol.*, 2015, pp. 34–36.
- [14] J. Y. Chyan and J. A. Yeh, "Return loss reduction of molded bonding wires by Comb capacitors," *IEEE Trans. Adv. Packag.*, vol. 29, no. 1, pp. 98–101, Feb. 2006.

- [15] H. R. Zhu, Y. F. Sun, and X. L. Wu, "Investigation of the capacitance compensation structure for wire-bonding interconnection in multichips module," in *Proc. IEEE Elect. Design Adv. Packag. Syst. Symp.*, Dec. 2017, pp. 1–3.
- [16] G. Liu, A. Trasser, A. Ç. Ulusoy, and H. Schumacher, "Low-loss, low cost, IC-to-board bondwire interconnects for millimeter-wave applications," in IEEE MTT-S Int. Microw. Symp. Dig., Jun. 2011, pp. 1–4.
- [17] C. H. Chan, C. C. Chou and H. R. Chuang, "Integrated packaging design of low-cost bondwire interconnection for 60-GHz CMOS vital-signs radar sensor chip with millimeter-wave planar antenna," *IEEE Trans. Compon. Packag.*, vol. 8, no. 2, pp. 177-185, Feb. 2018.
- [18] S. Beer *et al.*, "Design and measurement of matched wire bond and flip chip interconnects for D-band system-in-package applications," in *Proc. IEEE MTT-S Int. Microw. Symp.*, 2011, pp. 1–4.
- [19] S. Beer, H. Gulan, M. Pauli, C. Rusch, G. Kunkel, and T. Zwick, "122-GHz chip-to-antenna wire bond interconnect with high repeatability," in *IEEE/MTT-S Int. Microw. Symp. Dig.*, Jun. 2012, pp. 1–3.
- [20] M. Umar, M. Laabs, N. Neumann and D. Plettemeier, "Bondwire Model and Compensation Network for 60 GHz Chip-to-PCB Interconnects," *IEEE Antennas Wirel. Propag. Lett.*, vol. 20, no. 11, pp. 2196-2200, Nov. 2021.
- [21]S. D. Joseph and E. A. Ball, "Antenna Array and GaAs Phase Shifter MMIC for Millimeter wave Beamforming - Co-simulation and Measurements," in *Proc. EuCAP*, Glasgow, United Kingdom, 2024, pp. 1-5
- [22]E. A. Ball and S. D. Joseph, "Design and Measurement of a GaAs MMIC for use in a 73 GHz Time Modulated Array," in *Proc. IEEE CAMA*, Genoa, Italy, 2023, pp. 560-563.
- [23]E. A. Ball and S. D. Joseph, "A mmWave Transmitting Time Modulated Array Using Bespoke GaAs Integrated Circuits – Prototype Design and Laboratory Trials at 73 GHz," *IEEE Open J. Antennas Propag.*, early access article, 2024.
- [24] A. Bedda-Zekri and R. Ajgou, "Statistical Analysis of 5G/6G Millimeter Wave Channels for Different Scenarios," J. Commun. Technol. Electron., vol. 67, no. 7, pp. 854–875, 2022.
- [25]The National mmWave Measurement Laboratory. [Online]. Available: https://mmwave.group.shef.ac.uk.
- [26]C. R. Paul, Inductance: Loop and Partial. Hoboken, NJ, USA: Wiley, 2010



Sumin David Joseph (Member, IEEE) received the B.Tech. degree (Hons.) in electronics and communication from the CUSAT University, India, in 2012, M. Tech. degree (Hons.) in communication systems from the Visvesvaraya National Institute of Technology, India, in 2015, and dual PhD degree (distinction) in

electrical engineering from the University of Liverpool, U.K., and National Tsing Hua University, Taiwan in 2021.

Dr Sumin is currently working as a Post-Doctoral Research Associate with The University of Sheffield. He was a Lab Engineer under CoE with the Visvesvaraya National Institute of Technology, India from 2015 to 2017, where he was involved in projects of national importance.

Dr Sumin has authored or coauthored more than 40 articles in peer-reviewed journals and conference proceedings. His research interests include self-biased circulators, mm-wave antenna arrays, rectifying antennas, MMIC circuits, RFIC, rectifiers, integrated circuit designs, flexible electronics, wireless power transfer, energy harvesting and TMA antenna arrays. Dr Sumin is a technical reviewer for leading academic journals and conferences, including IEEE Transactions of Antenna and Propagation, IEEE Antenna and Wireless Propagation Letters and IEEE Access.



Edward A. Ball (M 2008 – SM 2024) Edward (Eddie) became a Member of IEEE in April 2008 and was born in Blackpool, United Kingdom in November 1973. Eddie graduated in 1996 with a 1st Class Master of Engineering Degree in Electronic Systems Engineering, from the University of York, York, United Kingdom. In 2024

he received a Ph.D. in RF Electronic Engineering from the University of Sheffield, Sheffield, United Kingdom.

After graduating in 1996, he worked in industry for 20 years, first spending 15 years working as Engineer, Senior RF Engineer and finally Principal RF Engineer at Cambridge Consultants Ltd in Cambridge, UK. He then spent 5 years as Principal RF Engineer and Radio Systems Architect at Tunstall Healthcare Ltd in Whitley, UK. In November 2015 he joined the Department of Electronic and Electrical Engineering at the University of Sheffield, Sheffield, United Kingdom, where he now works as Professor of RF Engineering. He is the group leader of the Electromagnetics, Wireless Hardware and RF Devices Group. His research interests cover all areas of radio technology, from RF system design, RF circuit design (sub GHz to mm-wave) and the application of radio technology to realworld industrial and commercial problems. He has a particular passion for RF hardware design. Professor Ball is a member of the IET and is a Chartered Engineer.